1 **Title: Evaluating the efficacy of protein quantification methods on membrane**
2 **proteins.**

3 **Authors:** Jana Löptien[1*], Sidney Vesting[1*], Susanne Dobler[1+], Shabnam Mohammadi[1,2+]

4 **Affiliations:**

5 1. Molecular Evolutionary Biology, Institute of Cell and Systems Biology of Animals, Universität
6   Hamburg, Hamburg, Germany
7 2. Max Planck Institute for Chemical Ecology, Jena, Germany

8 **Correspondence to:** smohammadi@ice.mpg.de and susanne.dobler@uni-hamburg.de

9 [*]Co-first authors

10 [+]Co-senior authors

11 **Keywords**: Protein quantification; transmembrane proteins; Na,K-ATPase, ELISA

12

13 **Abstract**
14 Protein quantification is an important tool for a wide range of biological applications. The most
15 common broadscale methods include the Lowry, bicinchoninic acid (BCA), and Coomassie Bradford
16 assays. Despite their wide applicability, the mechanisms of action imply that these methods may not
17 be ideal for large transmembrane proteins due to the proteins' integration in the plasma membrane.
18 Here, we investigate this problem by assessing the efficacy and applicability of these three common
19 protein quantification methods on a candidate transmembrane protein – the Na,K-ATPase (NKA). We
20 compared these methods to an ELISA, which we newly developed and describe here for the
21 quantification of NKA. The use of a relative standard curve allows this ELISA to be easily adapted to
22 other proteins and across the animal kingdom. Our results revealed that the three conventional
23 methods significantly underestimate the concentration of NKA compared to the ELISA. Further, by
24 applying the protein concentrations determined by the different methods to in vitro assays, we found
25 that variation in the resulting data was consistently low when the assay reactions were prepared based
26 on concentrations determined from the ELISA. Thus, when target protein concentrations vary across
27 samples, the conventional quantification methods cannot produce reliable results in downstream
28 applications. In contrast, the ELISA we describe here consistently provides robust results.
29
30 **1. Introduction**

31

32 Many biological applications rely on protein quantification. These include biochemical assays that
33 assess the function of proteins [1,2], the assessment of protein abundances between tissues and
34 species [3], and the assessment of knockdown experiments [4]. The most common all-encompassing
35 methods of protein quantification include the Lowry, bicinchoninic acid (BCA), and Coomassie Bradford
36 assays [5–7]. In general, these methods are sensitive, simple, inexpensive, and easily reproducible [8].
37 Moreover, they are available as standardized commercial kits. In all three methods, total protein
38 concentration is detected by a color signal whose intensity correlates with the quantity of total protein
39 present in the sample and which can be measured spectrophotometrically.

40

41 Both the Lowry and BCA assays are copper-based quantification methods. They rely on the reduction
42 of cupric ions (Cu^{2+}) to cuprous ions (Cu^+) – a process known as the biuret reaction. This reaction is
43 facilitated by the peptide bonds of proteins and the subsequent biuret signal formed intensifies in
44 proportion to the amount of Cu^+ in the sample [5,6,9]. Therefore, the more peptide bonds are

1

45 accessible to Cu^{2+} in the reaction, the stronger the biuret signal, and thus the higher the determined
46 protein concentration will be.

48 In the Lowry assay, a strong alkaline cupric sulfate and tartrate reagent is added to the protein sample
49 and during a short incubation, light blue tetradentate Cu^+ complexes form (the biuret reaction). These
50 complexes are formed between Cu^{2+} and the nitrogen atoms present in the peptide bonds of proteins.
51 In a secondary reaction, Cu^{2+} is reduced to Cu^+ by the protein peptide bonds (oxidation of peptide
52 bounds) [5,9]. Following incubation, the yellow Folin-Ciocalteu reagent (phosphotungstic acid and
53 phosphomolybdic acid mixture in phenol) is added and color strengthening occurs. The precise
54 mechanism for color strengthening using the Folin-Ciocalteu reagent is not completely understood,
55 but it is believed to occur when the tetradentate Cu^+ complexes transfer electrons to the
56 phosphomolybdic-phosphotungstic acid complexes (Cu^+ is oxidized back to Cu^{2+} by Mo^{6+}) [10]. The
57 reduced phosphomolybdic-phosphotungstic acid complexes produced by this reaction are intensely
58 blue in color (heteropolymolybdenum Blue (Mo^{5+})) and can be measured spectrophotometrically at
59 around 750 nm [5]. Some specific amino acids (tryptophan, tyrosine, and cysteine) also contribute to
60 the color strengthening by the Folin-Ciocalteu reagent [11]. Thus, proteins with higher frequency of
61 these amino acids will produce stronger color signals.

63 The BCA is a modification of the Lowry assay. BCA replaces the Folin-Ciocalteu reagent to generate a
64 method that is more tolerant to interference by commonly encountered substances present in protein
65 samples [6]. The advantage of the BCA is that it is relatively stable under alkaline conditions, unlike the
66 Lowry assay. Thus, BCA can be incorporated into the alkaline copper solution in a simplified one-step
67 procedure [6,12]. At room temperature, the readily oxidizable tryptophan, tyrosine, and cysteine or
68 cystine are the main amino acids responsible for Cu^{2+} reduction in this assay. At higher temperatures
69 (37-60°C), Cu^{2+} is also reduced by protein peptide bonds [6,13]. However, experiments with di-, tri- and
70 tetrapeptide proteins suggest that the extent of color formation is caused by more than the mere sum
71 of individual color-producing functional groups in the protein and that the peptide backbone likely
72 contributes as well [13]. In the final step of the reaction, each reduced Cu^+ chelates with two molecules
73 of BCA, forming a purple complex that can be measured spectrophotometrically at around 562 nm
74 [6,14].

76 In contrast to the Lowry and BCA assays, the Coomassie Bradford protein assay (Bradford assay) is
77 based on the binding of the Coomassie Brilliant Blue G-250 dye to protein, which results in protein-dye
78 complexes [7]. The Bradford assay is the fastest and simplest of all protein quantification methods. The
79 strong non-covalent binding of the dye to proteins is due to interactions with hydrophobic amino acids
80 tryptophan and phenylalanine and the polar amino acid tyrosine. The binding of the neutral species to
81 proteins also occurs due to electrostatic attraction between the negatively charged sulfonic group of
82 dye and the positively charged guanidino group of arginine and, to a lesser degree, of the other basic
83 amino acids, lysine and histidine. Protein-bound dye molecules shift their absorbance maximum near
84 615 nm [15], and the increase in absorbance around that wavelength is proportional to the number of
85 bound dye molecules [7].

87 All three conventional protein quantification methods have advantages and drawbacks. One of the
88 clear drawbacks is that they detect all proteins in a given sample and can thus only provide an estimate
89 for specific protein concentrations when samples contain unpurified or partially purified proteins.
90 Moreover, all three methods exhibit some degree of detection variation towards different protein
91 types (protein-to-protein variation). This can be attributed to the different reagents' affinities towards
92 certain amino acids, as described above. Indeed, the determined protein concentrations can be
93 significantly over- or underestimated depending on the amino acid composition of the proteins [16],
94 with the Bradford assay showing approximately twice as much detection variability compared to the
95 copper-based protein quantification methods [14]. The BCA and Lowry assays appear to have very
96 similar detection variability between different proteins [6].

97
98 Another limitation of these conventional methods is that the proteins must be solubilized to interact
99 with the assay reagents. This makes the methods susceptible to interference from other substances
100 present in protein samples. For example, the Bradford assay is sensitive to surfactants and detergents
101 (e.g., SDS or Triton X-100) at concentrations routinely used to lyse cells and solubilize membrane
102 proteins [7]. This is because detergents also bind to proteins and compete with the dye for binding
103 sites, thus preventing the color reaction [17]. The Lowry and BCA assays are compatible with most
104 surfactants, even if present in the protein sample at concentrations up to 1 % (Lowry assay) or 5 %
105 (BCA assay) [14]. On the other hand, the Bradford assay is less impacted by substances that reduce
106 copper (e.g., dithiothreitol or ß-mercaptoethanol) or copper-chelating agents (e.g., EDTA), which are
107 normally used to stabilize proteins in solution [7,12]. Buffer solutions that change the pH of the
108 reagents cause problems for all three conventional protein quantification methods. In general, the
109 Bradford assay is more tolerant towards interfering substances, like buffer salts, than the Lowry and
110 BCA assays [18], and the BCA assay is less prone to disruption than the Lowry assay [6,14]. In addition,
111 the Bradford reagent is highly acidic, thus, proteins with poor acid-solubility cannot be assayed with
112 this reagent.

113
114 Another challenge faced by these conventional methods, which we focus on here, is when proteins are
115 embedded in lipid membranes. Transmembrane proteins are largely embedded in the cell's
116 hydrophobic lipid bilayer, with one or more membrane-spanning regions that have hydrophobic amino
117 acid side chains distributed on their surface. Often, these transmembrane proteins have additional
118 hydrophilic domains located on the extra- and intracellular regions. Membrane proteins have proven
119 to be difficult to purify owing to their integration in the plasma membrane, partially hydrophobic
120 surfaces, flexibility, and lack of stability [19]. Moreover, some transmembrane proteins are only
121 present in low abundance, and it can be difficult to obtain enough protein for accurate quantification
122 [20]. The Bradford assay has already been shown to underestimate the protein concentration of
123 membrane-containing fractions due to the significant portion of membrane proteins being embedded
124 in the cell membrane and thus not accessible to the dye molecules [21]. Therefore, experimental work
125 with such proteins has often relied on relative protein quantification by a combination of Bradford
126 assays and western blots [22–26]. While these methods can be sufficient for estimating protein
127 concentrations across samples, they lack the precision needed for producing robust measurements,
128 especially when target protein concentrations vary across biological replicates. Moreover, western
129 blots are labor-intensive, and not ideal for explicit quantification.

130
131 Enzyme-linked immunosorbent assays (ELISAs) present a solution for quantifying large transmembrane
132 proteins and overcome some of the limitations and drawbacks associated with the conventional
133 methods. ELISAs are used to quantify specific target proteins in a sample. Thus, they overcome the
134 specificity limitations that conventional protein quantification methods face with heterogenous
135 protein samples. This specificity is achieved in ELISAs through antibody-antigen interactions and an
136 enzyme-mediated color reaction to detect the presence of the target protein (antigen). This interaction
137 allows the quantification of small amounts of a specific target protein in a heterogenous sample
138 [27,28]. However, due to their specificity, commercial ELISAs for less commonly studied proteins and
139 for proteins from non-model organism are hard to come by and cost prohibitive.

140
141 ELISAs follow the same basic principles [28,29]. The first step is adhering or immobilizing the target
142 protein from the liquid phase directly onto the surface of 96-well plate wells. Following this,
143 unsaturated surface-binding sites are blocked by non-reacting protein, such as bovine serum albumin
144 (BSA). Next, the target protein is detected either directly (enzyme-labeled primary antibody that binds
145 specifically to the target protein) or indirectly (such as enzyme-labeled secondary antibody that detects
146 the primary antibody-target protein interaction). In the final step, substrates for the enzyme are
147 introduced and enzymatically converted to a chromogenic, fluorescent, or luminescent signal. The
148 intensity of the signal directly correlates with the amount of target protein present in the sample.

149
150 Three types of ELISAs have been developed: sandwich, direct, and indirect. A sandwich ELISA is the
151 most precise method because the target protein is bound between two primary antibodies (capture
152 antibody and detection antibody), each detecting a different epitope of the target protein. However,
153 this method requires a lot of tailoring for each protein type and is thus not easily applicable across a
154 broad range of proteins. A direct ELISA uses a single primary antibody, which also serves as the
155 detection antibody, allowing the direct detection of the target protein. An indirect ELISA relies on a
156 secondary antibody to detect the primary antibody. A standard secondary antibody can be applied to
157 different primary antibodies, and the primary antibody does not require any labeling. The indirect
158 ELISA is thus the most easily applicable method. Although a variety of commercial ELISA kits are
159 available for different proteins, they are expensive, specific for only a narrow range of protein sources
160 (e.g., rats, mice, humans) and can be ineffective depending on the protein isolation methods.
161
162 To address the challenge of accurate transmembrane protein quantification, we compare the three
163 conventional methods (Lowry, BCA, and Bradford) and evaluate their performance in detecting and
164 quantifying transmembrane proteins in comparison to an indirect ELISA, which we newly developed
165 and validate here. We use Na, K-ATPase (NKA) as our model protein. This transmembrane protein has
166 been studied extensively in our working group and we have established a high-throughput expression
167 system to produce NKA from a wide range of taxa. The smallest functional unit of the NKA consists of
168 a dimer of a large α-subunit with 10 transmembrane helices and a glycosylated β-subunit of one
169 transmembrane helix [30,31].
170
171 The ELISA developed for NKA in this paper makes use of a commercially available primary antibody,
172 which binds universally across the animal kingdom. Attempts to produce a standard from commercially
173 available purified NKA proved ineffective. Therefore, we additionally developed a method for
174 producing relative standards by lyophilizing an aliquot of the protein being measured. These
175 specifications allow our ELISA to be adapted to any protein type and source.
176
177
178 **2. Material and Methods**
179
180 All key resources and reagents used in this study are listed in detail in Table S1.
181
182 **Acquiring expression vectors**
183
184 The majority of our protein samples were produced by expression in cell culture. This allowed us to
185 sample from a broader range of taxa. We used six pFastBac Dual plasmids, which have two cloning
186 sites for the simultaneous expression of two proteins, containing the NKA α1- and β1-subunit genes
187 from six different animal species. The species included the brown rat (*Rattus norvegicus*), common
188 ostrich (*Struthio camelus*), gold tegu (*Tupinambis teguixin*), large milkweed bug (*Oncopeltus fasciatus*),
189 Miranda's white-lipped frog (*Leptodactylus macrosternum*), and red-necked keelback snake
190 (*Rhabdophis subminiatus*). We selected these species because we wanted to sample as broad a range
191 of animals as possible. All vertebrate vectors were originally produced by Mohammadi et al., [1,26,32]
192 and the large milkweed bug vector was produced by S. Dalla [32]. Each vector had the α1-subunit gene
193 (ATP1A1 for vertebrates, ATPα1C for the large milkweed bug) under the control of the P_{PH} promoter
194 and the β-subunit gene (ATP1B1 for vertebrates, β1 for the large milkweed bug) under the p_{10}
195 promoter. Accession numbers for the sequences and the Addgene plasmid numbers associated with
196 these plasmid constructs can be found in Table S2.
197
198 **Bacmid production**
199

4

200 The six recombinant plasmids were transposed into competent DH10Bac *Escherichia coli* cells and
201 grown on plates containing gentamycin, tetracycline, kanamycin, Isopropyl β-D-1-
202 thiogalactopyranoside (IPTG), X-Gal. DH10Bac cells contain a bacmid and a helper plasmid. The
203 transposed donor plasmid segment containing the inserted ATP1A1 and ATP1B1 genes, along with a
204 gentamicin resistance gene, recombines at the *lac*Z alpha peptide gene on the bacmid, disrupting its
205 reading frame. The resulting colonies are white when grown on plates containing IPTG and X-Gal,
206 whereas those with intact *lacZ* proteins, i.e., failed recombination, are blue. Following transposition,
207 two white colonies were picked from each plate (per NKA construct) and incubated in liquid culture
208 containing gentamycin, tetracycline, and kanamycin to amplify the recombinant bacmids.
209
210 The amplified bacmid DNA was isolated from *E. coli* cells via alkaline lysis. Briefly, the *E. coli* cells were
211 lysed with a strong alkaline solution consisting of 200 mM NaOH and 1% SDS. Cell debris, SDS, and
212 genomic DNA was removed by centrifugation, and the resulting bacmid DNA was pelleted and washed
213 with 70% ethanol. The pellet was resuspended in purified water and the resulting bacmid DNA was
214 analyzed by PCR and agarose gel electrophoresis to verify that the transposition of the genes of interest
215 to the bacmids was successful (Fig. S1). The primers used for this analysis were pUC/M13 FWD 5'-
216 CCCAGTCACGACGTTGTAAAACG-3' and pUC/M13 RVS 5'-AGCGGATAACAATTTCACACAGG-3'.
217

218 **Generation of recombinant baculoviruses and expression of NKA proteins in Sf9 cells**
219
220 Sf9 cells (immortalized ovary cells from the moth *Spodoptera frugiperda*) were used as the host for
221 recombinant baculovirus production and protein expression. Sf9 cells are advantageous for NKA
222 expression because they express very little of the protein endogenously [33,34].
223
224 We followed the modified one-step protocol described by Scholz and Suppmann [35]. For baculovirus
225 production, 8×10^6 Sf9 cells in 10 mL Insect-Xpress medium with 30 μg/mL gentamycin were transfected
226 with 10 μg purified bacmid DNA using PEI MAX. We repeated this procedure three times to produce
227 three biological replicates (A, B, C) per NKA construct. After 5 days of incubation at 27°C and 110 rpm,
228 the Sf9 cells were pelleted by centrifugation at 500 x g for 5 min and the P0 viruses in the supernatant
229 were harvested. Freshly seeded Sf9 cells (50×10^6 cells in 50 mL media) were subsequently infected with
230 the P0 viruses (500 μL virus per biological replicate). Following three days of incubation at 27°C and
231 110 rpm, the Sf9 cells were pelleted by centrifugation at 1650 x g for 10 min and stored at -80°C until
232 membrane isolation. Additionally, uninfected Sf9 cells (i.e., without NKA expression) were also
233 cultured (25×10^6 cells in 50 mL media) and pelleted for use as a negative control.
234

235 **Membrane isolation from Sf9 cells**
236
237 The frozen Sf9 cell pellets were resuspended in 15 mL of homogenization buffer (0.25 M sucrose, 2
238 mM EDTA, 25 mM HEPES; adjusted to pH 7.0 with Tris HCl) on ice. The cell suspensions were then
239 sonicated at 60 W (Sonopuls 2070) for three 45 s intervals on ice to lyse the cells and disrupt the cell
240 membranes. Next, the cell suspensions were centrifuged for 30 min at 10,000 x g and 4°C (Centrifuge
241 5840 R) to pellet cell debris. The supernatant was collected and further centrifuged for 60 min at
242 146,000 x g and 4°C (Ultra-Centrifuge L-80) to pellet the cell membranes. The supernatant was
243 removed, and the pelleted membranes were washed twice and resuspended in cooled HPLC grade
244 water (1 mL per biological replicate), then stored at -20°C.
245

246 **Preparation of tissue samples**
247
248 Brain and kidney tissue was dissected from three freshly frozen black rats purchased commercially
249 from frostmaus.de. Nervous tissue (brains, prothoracic and central ganglia) was also dissected out of
250 14 freshly frozen large milkweed bugs and pooled into one sample. The bugs were acquired from a
251 colony reared at University of Hamburg [36]. All tissue samples were homogenized on ice with a glass

5

252 grinder in 500 μL HPLC grade water. Nervous tissue samples were lyophilized overnight (12-24 h) at
253 0.1 mbar and -50°C in a freeze dryer. After lyophilization, the freeze-dried samples were reconstituted
254 in 500 μL (large milkweed bug) or 1 mL (black rat) cooled HPLC grade water. The reconstituted samples
255 were then sonicated in an ice bath for 10 min (Omni Sonic Ruptor 400, Pulser 90, Power 90%) and
256 centrifuged for 10 min at 5000 x g and 4°C (Centrifuge 5840 R) to precipitate debris. The resulting
257 supernatant was stored at -20°C. Membranes from kidney samples were isolated as described above
258 for Sf9 cells. Nervous tissue is known to have very high levels of NKA expression compared to other
259 tissues [37–40]. Therefore, we deemed it unnecessary to concentrate the proteins by isolating
260 membranes for this tissue.
261
262 **Positive control**
263
264 A lyophilized sample of commercially available, purified NKA from porcine cerebral cortex (0.3
265 units/mg protein; Table S1) was reconstituted to a stock concentration of 10 mg/mL in HPLC grade
266 water.
267
268 **Table 1.** List of protein samples used in this study. Protein samples derived from tissue are highlighted
269 in grey, all others were expressed in Sf9 cells.
270

Order	Species	NKA Source	Used for
Mammalia	*Rattus norvegicus* (brown rat)	Expressed in Sf9 cells	(1) testing effects of lyophilization (2) relative NKA standard production (3) comparing protein quantification methods (4) comparing applicability of quantification methods
Mammalia	*Rattus rattus* (black rat)	Brain tissue preparation	(3) comparing protein quantification methods (4) comparing applicability of quantification methods
Mammalia	*Rattus rattus* (black rat)	Kidney tissue preparation	(3) comparing protein quantification methods (4) comparing applicability of quantification methods
Mammalia	*Sus domesticus* (porcine)	Commercially available, lyophilized cerebral cortex NKA isolate	(2) NKA standard production (3) comparing protein quantification methods – **positive control**
Aves	*Struthio camelus* (common ostrich)	Expressed in Sf9 cells	(1) testing effects of lyophilization (2) relative NKA standard production (3) comparing protein quantification methods (4) comparing applicability of quantification methods
Squamata	*Tupinambis teguixin* (gold tegu)	Expressed in Sf9 cells	(1) testing effects of lyophilization (2) relative NKA standard production (3) comparing protein quantification methods (4) comparing applicability of quantification methods
Squamata	*Rhabdophis subminiatus* (red-necked keelback snake)	Expressed in Sf9 cells	(1) testing effects of lyophilization (2) relative NKA standard production (3) comparing protein quantification methods (4) comparing applicability of quantification methods
Amphibia	*Leptodactylus macrosternum* (Miranda's white-lipped frog)	Expressed in Sf9 cells	(1) testing effects of lyophilization (2) relative NKA standard production (3) comparing protein quantification methods
Insecta	*Oncopeltus fasciatus* (large milkweed bug)	Expressed in Sf9 cells	(1) testing effects of lyophilization (2) relative NKA standard production (3) comparing protein quantification methods (4) comparing applicability of quantification methods

6

Insecta	*Oncopeltus fasciatus* (large milkweed bug)	Brain and ganglia tissue preparation	(3) comparing protein quantification methods
Insecta	untransfected Sf9 cells (ovary cells from *Spodoptera frugiperda*)	Sf9 cells (contain very little to no endogenous NKAs)	(1) testing effects of lyophilization (3) comparing protein quantification methods – **negative control**

271
272
273 **Testing the effect of lyophilization on antibody detection**
274
275 We wanted to prepare relative standards for our ELISA by using the dry weight of lyophilized protein
276 samples containing NKA from different species. We therefore first tested whether lyophilizing NKA
277 would cause a reduction in their detection by antibodies. For this comparison we used a 300 µL aliquot
278 of membrane isolated samples derived from Sf9 cell expression (Table 1), which consisted of 100 µL of
279 each replicate (A-C) pooled together. For common ostrich and Miranda's white-lipped frog, 162.5 µL
280 of replicates A and B were pooled because the C replicates were contaminated during the preparation
281 process. The samples were dried overnight (12-24 h) at 0.1 mbar and -50°C in a freeze dryer.
282 Afterwards, the samples were centrifuged shortly and their weights calculated by subtracting the
283 weight of the empty tubes. The freeze-dried samples were then reconstituted in 200-300 µL cooled
284 HPLC grade water. An aliquot was taken from each sample for the downstream production of relative
285 standards.
286
287 For the western blot analysis, 2.5 µL of non-lyophilized and reconstituted lyophilized samples were
288 solubilized in 8 µL 4x Laemmli buffer (62.5 mM Tris HCl pH 6.8; 2 % SDS; 10 % glycerol; 5 % 2-
289 mercaptoethanol; 0.001 % Bromophenol Blue) and 21.5 µL Millipore water. The solubilized samples
290 were then separated on an SDS gel containing 10% acrylamide. Subsequently, the separated proteins
291 were blotted from the gel onto nitrocellulose membrane. To block unsaturated binding sites on the
292 membranes after blotting, they were incubated at room temperature in 1x BlueBlock PF on a plate
293 tipper at medium tipping speed for 1 h. After blocking, the membranes were transferred into a 50 mL
294 Falcon tube and incubated with 2 mL of the primary antibody (Table S1) at a concentration of 0.88
295 µg/mL in 1x BlueBlock PF overnight at 4°C on a tube rotator. Next, the membranes were washed three
296 times with 1x BlueBlock PF. The membranes were then incubated with 2 mL of the secondary antibody
297 (Table S1) at a concentration of 8 µg/mL in 1x BlueBlock PF for 1 h at room temperature on the tube
298 rotator. Next, the membranes were washed three times with 1x BlueBlock PF and two additional times
299 with 0.05 M Tris HCl for 5 min each. The antibody complexes were stained by moving the membranes
300 into a glass petri dish and adding the detection enzyme substrate (0.035 % H_2O_2, and 0.01 % 4-Chloro-
301 1-naphthol in 0.05 M, pH 7.5 Tris HCl). Following a 10 min incubation, the staining reaction was stopped
302 by washing the membrane with deionized water. The resultant membranes were scanned (Canon
303 9000F Mark II). These samples were also compared on our ELISA (described below) and the results
304 from both the western blot and ELISA were statistically compared (described below). See Table S3 for
305 raw data.
306
307 **Protein assays**
308
309 All the protein samples we produced were quantified by Lowry, BCA, Bradford, and ELISA. The
310 commercial porcine sample was used as a positive control, and the protein sample derived from
311 untransfected Sf9 cells was used as a negative control. All four assays were run on aliquots that were
312 not previously freeze-thawed.
313
314 **Lowry protein assay**
315
316 We used Thermo Fisher Scientific's Modified Lowry protein assay kit (Table S1). First, a standard curve
317 was prepared with bovine serum albumin (BSA) (1500, 1000, 750, 500, 250, 125, 25, 5, 1, and 0 µg/mL)

318 in Millipore water. The protein samples were diluted 1:10 in Millipore water, except for porcine and
319 large milkweed bug tissue samples, which were not diluted because low protein content was expected
320 in these samples. 40 µL of the standards and protein samples were pipetted in duplicate (two technical
321 replicates) into 96-well polystyrene flat-well plate wells. 200 µL of Lowry reagent was added to each
322 well, mixed on a microplate shaker for 30 seconds, and then incubated at room temperature for 10
323 min. Following incubation, 20 µL of freshly prepared 1x Folin-Ciocalteu reagent was added to each well
324 and mixed on the microplate shaker for 30 seconds. Following a 30 min room temperature incubation,
325 the absorbance of standards and protein samples was measured at 655 nm using a microplate
326 absorbance reader (Bio-Rad Model 680). See Table S4 for raw Lowry assay data.
327
328 **Bicinchoninic acid (BCA) protein assay**
329
330 We used Thermo Fisher Scientific's Bicinchoninic acid protein assay kit (Table S1). First, a standard
331 curve was prepared with BSA (1500, 1000, 750, 500, 250, 125, 25, 5, 1, and 0 µg/mL) in Millipore water.
332 The protein samples were diluted 1:10 in Millipore water, except for porcine and large milkweed bug
333 tissue samples, which were not diluted. 25 µL of the standards and protein samples were pipetted in
334 duplicate (two technical replicates) into 96-well polystyrene flat-well plate wells. 200 µL of freshly
335 prepared, clear, green BCA working reagent was added to each well, and mixed on a microplate shaker
336 for 30 seconds. Following a 30 min incubation at 37°C and subsequent cooling of the plate to room
337 temperature, the absorbance of standards and protein samples was measured at 550 nm using a
338 microplate absorbance reader (Bio-Rad Model 680). See Table S5 for raw BCA assay data.
339
340 **Coomassie Bradford protein assay**
341
342 For the Bradford assay, we prepared a standard curve with BSA (10, 8, 6, 4, 2, and 0 µg/mL) in Millipore
343 water. The protein samples derived from Sf9 cells and rat brain tissue were diluted 1:2000 in Millipore
344 water, whereas porcine and large milkweed bug tissue samples were diluted 1:200 (see methods
345 above). Both the standards and protein samples were then diluted 1:2 with Coomassie Bradford
346 reagent and pipetted into polystyrene cuvettes in duplicate (two technical replicates). After incubating
347 at room temperature for 10 mins, the absorbance of standards and protein samples was measured at
348 595 nm using a cuvette spectrophotometer (Ultrospec 2100 pro). See Table S6 for raw Bradford assay
349 data.
350
351 **Relative NKA standard preparation for the ELISA**
352
353 For each animal species to be assayed, a relative NKA standard was prepared from the lyophilized
354 membrane isolates derived from Sf9 cells (Fig. 1). The concentration of each standard was calculated
355 based on their lyophilized weights (described above). These concentrations were used to create
356 relative NKA standard stock aliquots of 1 mg/mL in ELISA coating buffer (0.1 M NaHCO$_3$ in PBS, adjusted
357 to pH 9.5 with KOH; Table S7) for each animal species.
358
359
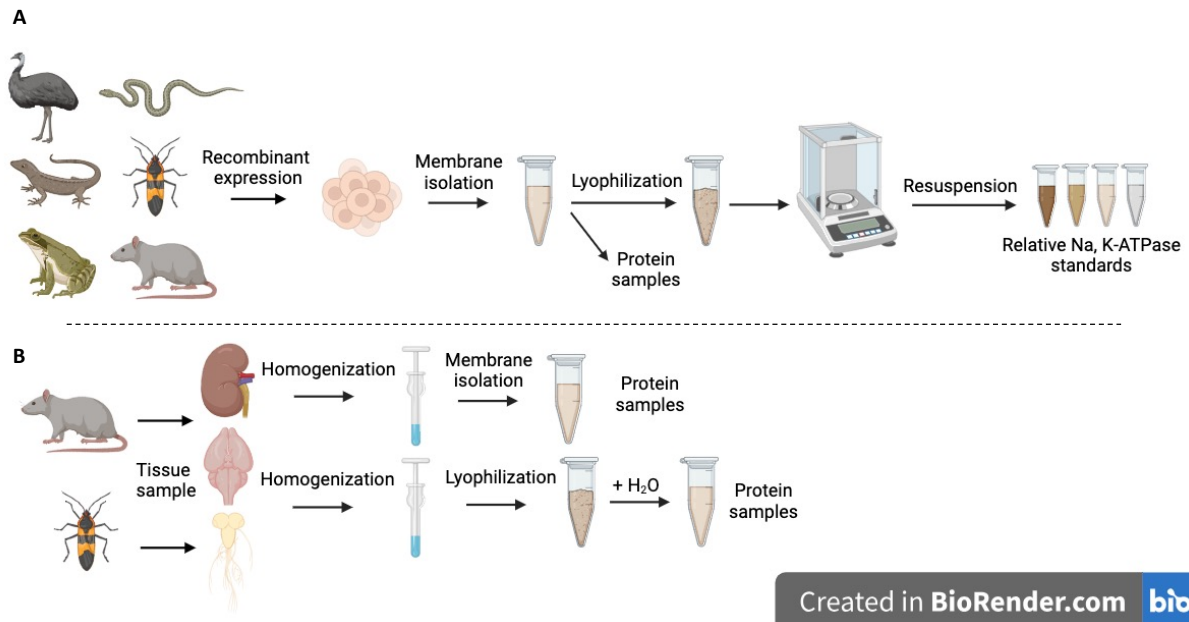
Figure 1. Schematic diagram illustrating the isolation of proteins from (A) recombinant expression in Sf9 cells and (B) from tissues. Nervous tissue samples were isolated by homogenization, followed by centrifugation to pellet waste and lyophilization, whereas all other samples were membrane isolated. Relative Na, K-ATPase (NKA) standards were subsequently prepared from a subset of membrane isolates from recombinantly expressed Sf9 cells. All resulting protein samples were used in all four quantification assays, while the relative NKA standards were produced specifically for the ELISA. Figure created with BioRender.com.

Indirect ELISA to quantify NKA proteins

Prior to running an ELISA, the protein samples were diluted 1:2000 in the coating buffer (Table S7). Replicates A-C of common ostrich and large milkweed bug were diluted 1:6000 and 1:4000, respectively, because higher NKA concentrations were expected in these samples based on the western blots. The 1 mg/mL relative NKA standard stocks were sonicated in an ice bath for two 2.5-min intervals (Omni Sonic Ruptor 400, Pulser 90, Power 90%) and afterwards the standards were diluted in coating buffer to the following concentrations: 60, 30, 20, 15, 10, 7.5, 5, 3.75, 2.5, 1.875, 1.25, 0.9375, 0.625, and 0 µg/mL. All ELISAs were run on aliquots that were not previously freeze-thawed.

First, 100 µL of protein samples and relative NKA standards were added to 96-well polystyrene flat-well plates in duplicate (two technical replicates). Additionally, 100 µL of a negative control using only coating buffer without any protein was added to the plates. This negative control is equal to the 0 µg/mL standard. After adding samples and standards to the wells, the plates were sealed with Parafilm® and incubated overnight at 4°C (12-18 h).

The next day, unbound leftovers were discarded and plates dried by tapping them several times face-down on a paper towel. Each well was washed by adding 400 µL of washing buffer (0.05 % Tween® 20 in PBS; Table S7), letting it sit for 10 s, then discarding fluids as described above. This washing procedure was repeated to a total of five times. Next, unsaturated surface-binding sites were blocked by adding 200 µL of blocking buffer (1 % BSA, 0.02 % Tween® 20 in PBS; Table S7) to each well, sealing the plates with Parafilm®, and incubating at room temperature for 2 h. Following blocking, the wells were washed as described above.

394
395 We used the universal monoclonal primary antibody α5 to detect the NKA α-subunit (α5-antibody;
396 Table S1). The antigen species for this antibody is chicken and the host species is mouse. The α5-
397 antibody binds a cytosolic epitope on the α-subunit of all NKA isoforms across the animal kingdom. 50
398 μL of primary antibody solution containing 2 μg/mL α5-antibody in blocking buffer was added to each
399 well, and left to incubate, sealed with Parafilm®, for 1 h at room temperature (overnight (12-18 h) at
400 4°C is also possible).
401
402 To remove unbound primary antibodies, the wells were washed as described above. Next, we used a
403 goat-anti-mouse polyclonal secondary antibody conjugated with horseradish peroxidase (HRP-
404 antibody; Table S1) to detect the primary antibody. The host species for the secondary antibody is
405 goat. 50 μL of secondary antibody solution containing 5 μg/mL HRP- antibody in blocking buffer was
406 added to each well, and left to incubate, sealed with Parafilm®, for 1 h at room temperature.
407
408 Following the secondary antibody incubation, each well was washed seven times as described above
409 to maximally reduce background noise caused by unbound HRP-antibody. The colorimetric reaction of
410 HRP was triggered by adding 100 μL 3,3',5,5'-tetramethylbenzidine (TMB) to each well, and allowing
411 color development at room temperature for 10 min. The colorimetric reaction was stopped by adding
412 100 μL stopping solution (0.5 M H_2SO_4) to each well. Finally, the absorbance of standards and protein
413 samples was measured at 490 nm using a microplate absorbance reader (Bio-Rad iMark™). See Fig. 2
414 for a schematic diagram of the ELISA methods and Table S7 for buffer recipes.
415
416
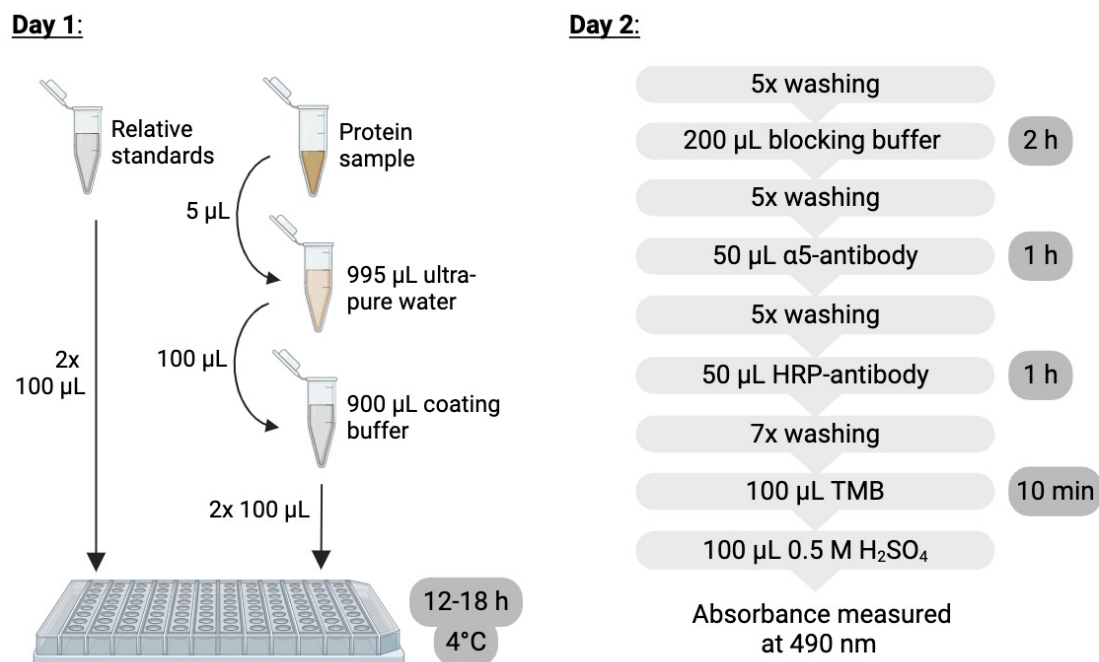
417
418
419
420 **Figure 2.** Schematic diagram illustrating the two-day ELISA procedure. Figure created with
421 BioRender.com.
422
423 **Negative controls**
424

425 Several negative controls were included to validate the functionality of this ELISA. First, the primary
426 antibody (α5-antibody) was omitted to confirm that there is no non-specific binding of the secondary
427 HRP-antibody. Next, the HRP-antibody was omitted to confirm that TMB and the stopping solution do
428 not stain non-specifically (i.e., without HRP). For these negative controls, a random sample from our
429 Sf9 expressed proteins was used (gold tegu replicate A). Then, both protein and antibodies were
430 omitted to confirm that there is no background noise caused by the buffers. Finally, membrane isolate
431 of uninfected Sf9 cells was run in the ELISA to confirm that the antibodies are not binding non-
432 specifically to other membrane proteins. See Table S8 for raw negative control data.
433
434 **Calculation of protein concentrations**
435
436 For all protein quantification methods, the average absorbance of the two blank standard replicates
437 (0 μg/mL) was subtracted from each absorbance measurement. Then, the average values of the two
438 technical replicates were calculated. The average absorbance values of each standard were used for a
439 linear trendline-fitting. For the ELISA, either the entire range up to 60 μg/mL (red-necked keelback
440 snake, commercial porcine NKA) or concentrations ranging from 0 to 10, 20, or 30 μg/mL were used,
441 depending on the extent of the linear range of the standard curves. The resulting linear equations were
442 used to calculate the protein concentrations of the samples. See Table S9 for raw ELISA data.
443
444 **Testing the robustness of protein quantification methods with in vitro NKA activity assays**
445
446 To examine the robustness of the determined protein or NKA concentrations, the variation across
447 biological replicates of in vitro NKA activity assays were compared. Only animal species with three or
448 more biological replicates were tested in the NKA activity assays. Thus, Miranda's white-lipped frog
449 and large milkweed bug tissue were excluded from the assays. Replicate C of Miranda's white-lipped
450 frog encountered infection problems during transfection whereas the number of large milkweed bugs
451 we dissected was only sufficient to produce only one biological replicate for the tissue. For each assay,
452 100 μg of protein was used and this was calculated based on concentrations determined by the four
453 different protein quantification methods. The 100 μg of protein was pipetted in duplicate (two
454 technical replicates) into two wells on a 96-well polystyrene flat-well plate. The first well contained
455 stabilizing buffer to measure total ATPase activity and the second well contained inhibiting buffer
456 (lacking KCl and including 10^{-2} M ouabain) to block NKAs and measure background ATPase activity. See
457 assay buffer formulas in Petschenka et al. [41]. The proteins were incubated at 37°C and 200 rpms for
458 10 min on a microplate shaker.
459
460 Next, ATP (10 mM Tris-ATP, pH 6.5) was added to each well and the proteins were incubated again at
461 37°C and 200 rpms for 20 min. The activity of NKAs was determined by quantification of inorganic
462 phosphate (P_i) released from enzymatically hydrolyzed ATP. Reaction P_i levels were measured
463 according to the procedure described by Petschenka et al. [41]. The reactions were stopped with 10 %
464 SDS and then stained with a solution consisting of Taussky-Shorr color reagent [42], which turned the
465 reactions blue in proportion to their P_i concentration. After 10 min of staining, the absorbance of each
466 well was measured at 655 nm using a microplate absorbance reader (Bio-Rad Model 680). Average
467 absorbance values of the two technical replicates were used for subsequent calculations.
468
469 The averages of two technical replicates were translated to mM P_i based on a standard curve of KH_2PO_4
470 (0 - 1.2 mM P_i) that was run on the same plate. Background ATPase P_i concentrations were subtracted
471 to obtain NKA ATPase P_i concentrations [41]. The P_i concentrations released from 100 μg of protein
472 were then converted to nmol P_i/(mg protein*min).
473
474 **Statistical analyses**
475

476 To test whether lyophilization alters NKA detection by antibodies, we compared the distribution of
477 ELISA absorbance values between lyophilized and non-lyophilized samples with a Wilcoxon signed-
478 rank test for paired samples. In addition, we compared the densities of the western blot's NKA α-
479 subunit bands (~110 kDa) between the two treatments using ImageJ 1.53k to draw plots from the
480 signal strength and size of the western blot bands. From the resulting plots, the areas under the curves
481 were calculated [43]. We then compared the distribution of the areas under the curves between
482 lyophilized and non-lyophilized samples with a Wilcoxon signed-rank test for paired samples. For both
483 analyses, the values for all samples were pooled together based on the treatment.

485 We used a Friedman rank sum test for paired samples to compare the NKA detection capabilities of
486 the four different quantification methods. We first compared the concentration values between Sf9
487 and tissue derived samples and found a significant difference (Wilcoxon paired test; $p < 0.0001$). We
488 thus continued by analyzing Sf9 and tissue derived samples separately. The positive control
489 (commercial porcine sample), the negative control (uninfected Sf9 cells), and replicate C of Miranda's
490 white-lipped frog (which was infected by bacteria in cell culture) were excluded from this analysis. For
491 the remaining, determined protein concentrations of different samples were pooled for each
492 quantification method respectively. A two-sided Dunn's post hoc test (R package "rstatix" [44]) was
493 used to identify the quantification methods that significantly differ from one another in the distribution
494 of their determined protein concentrations. Since multiple pairwise comparisons were performed
495 simultaneously in this test, the Bonferroni adjustment method was used for controlling the family-wise
496 error rate.

498 To evaluate the robustness of the determined NKA concentrations across the four methods, a one-way
499 analysis of variance (ANOVA) was used to compare the mean variation (scatter) in NKA activities
500 (specified by standard deviation of ATPase activity) across the three biological replicates (A, B, C). The
501 NKA activity assays were based on 100 µg of protein calculated from concentrations determined by
502 the four quantification methods. In the ANOVA, animal species was considered a random effect. Also,
503 standard deviations and coefficients of variation of different animal species were pooled for each
504 quantification method respectively. A power analysis (R package "pwr" [45]) revealed high power (>99
505 %) of the ANOVA to detect true effects or differences in the data. The black rat brain and kidney tissue
506 samples were excluded from the analysis, because the amount of P_i released from these samples was
507 beyond the linear range of the P_i standard curve. Despite running several additional rounds with more
508 diluted samples, we were never able to capture an activity range within the P_i standards before using
509 up the tissue samples.

511 All statistical analyses were performed using R 4.1.1 software (R Core Team, 2021) and a significance
512 level of 0.05 was applied. See Supplementary Dataset 1 for data table used for statistical comparisons.

514 **3. Results**

516 **Lyophilization does not affect NKA detection by antibodies**

518 To test whether lyophilization affects the detection of NKA by the ELISA antibodies, we compared Sf9
519 membrane isolates that were lyophilized to their non-lyophilized counterparts on a western blot (Fig.
520 3A) and in the ELISA. We analyzed the distribution of the western blot band densities and found no
521 significant difference between lyophilized and non-lyophilized samples (Wilcoxon signed-rank paired
522 test; $p = 0.81$; W = 16; n = 7; Fig. 3B). The ELISA corroborated the same result (Wilcoxon signed-rank
523 paired test; $p = 0.08$; W = 25; n = 7; Fig. 3B); showing no significant difference in the distribution of the
524 absorbance values between the two treatments. These results confirm that lyophilization of Sf9 cell
525 membrane isolates does not significantly diminish the detectability of the NKA proteins by the
526 antibodies used in the ELISA.

527
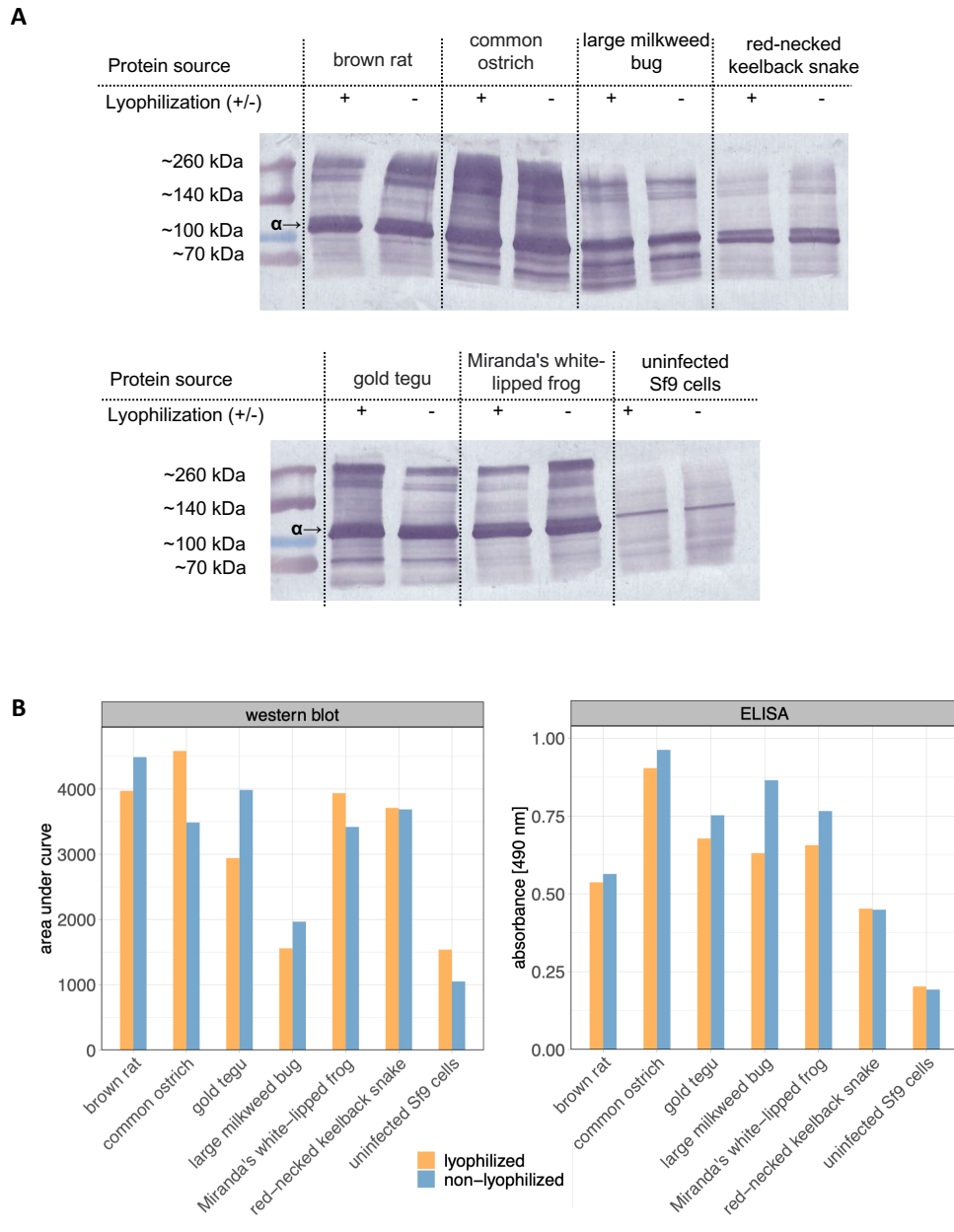
Figure 3. (A) Western blot membrane scans show lyophilized and non-lyophilized Sf9 cell membrane isolates run on two gels. The 110 kDa line corresponds to the NKA's α-subunit, which is marked by an arrow. Because the α5 primary antibody is specific only to the NKA α-subunit, additional bands and smearing are most likely caused by higher order complexes and high protein load. The + and − indicate which bands are lyophilized (+) and which are not (−). (B) Comparison of detection intensity between lyophilized and non-lyophilized Sf9 membrane isolates in the western blot and ELISA analyses. Densities of the western blot's NKA α-subunit bands were determined by the areas under the curves in ImageJ (Fig. S3; Table S3).

Relative NKA standard curves vary between different animal species

Because the α5 antibody can have different binding affinities to NKA from different animals, we produced a standard curve for each species. These standards were prepared from NKA expressed in Sf9 cells for consistency and reproducibility. In addition, we prepared standards from commercial porcine NKA. We found that most standard curves reached saturation well before the higher

13

concentration range (0 µg/mL to 60 µg/mL; Fig. 4A). Omitting the saturated range allowed us to capture the linear range needed for appropriate concentration calculations (Fig. 4B). The red-necked keelback snake standard was an exception to this pattern, for which a linear curve fit over the entire range of standards (Fig. 4A) – this is likely due to it having very low levels of NKA expression and thus lower amounts of NKA per mg lyophilized membrane isolate (Fig. S2). The standards prepared from commercial porcine NKA exhibited similarly low detectability by the α5 antibody. This was, however, surprising because the commercial porcine sample contains only NKA in membrane fragments and thus each mg is pure NKA. Because of the high variation, having standards tailored to each animal group ensures that the concentrations of samples are not over- or underestimated in the ELISA.
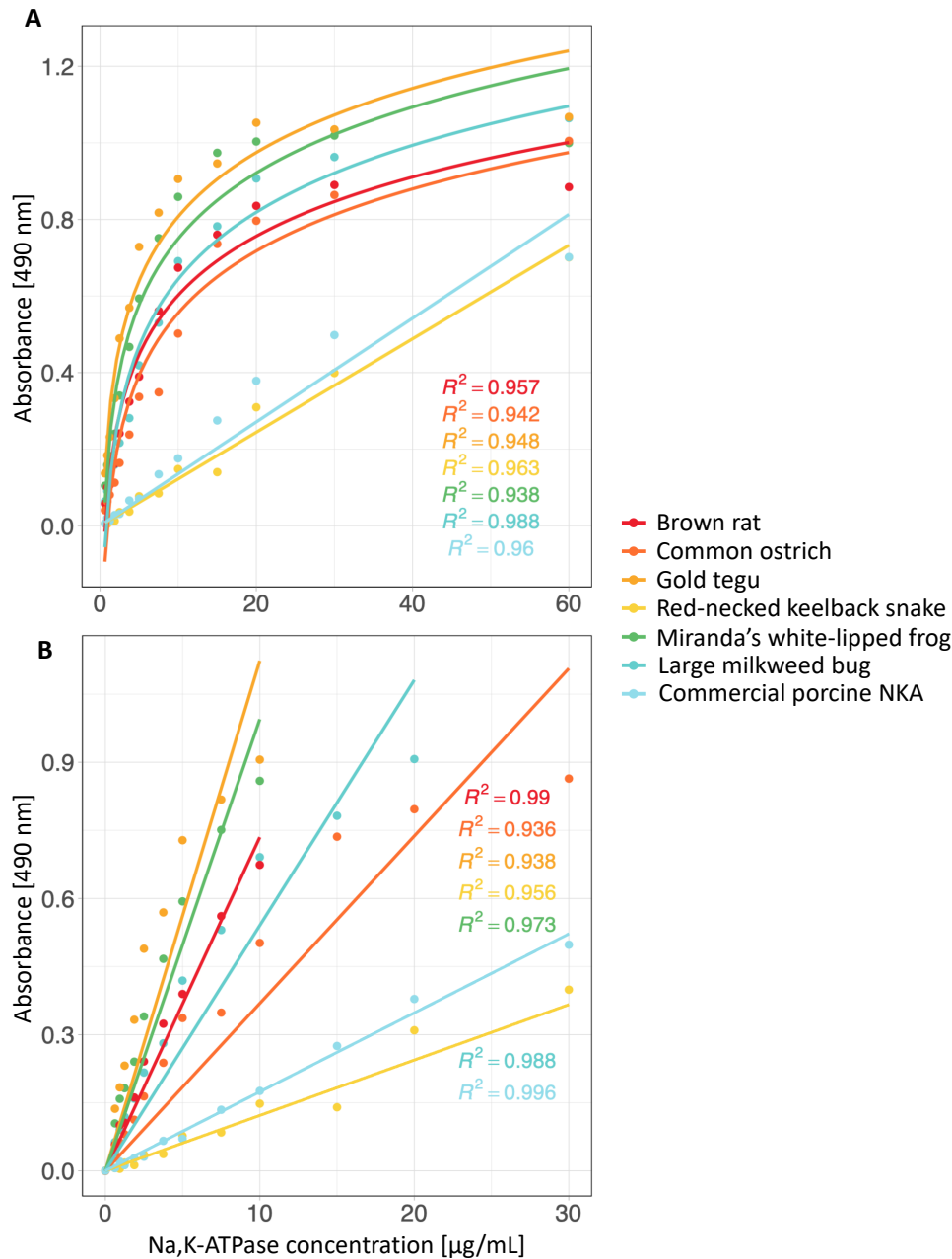

Figure 4. Comparison of standard curves generated from Sf9 cell membrane isolates containing recombinantly expressed Na, K-ATPase (NKA) from different animal species. Additionally, a standard curve prepared from purified commercial porcine NKA is included. (A) The full range of the relative

14

NKA standards (0 to 60 μg/mL) reached saturation mid-way for most animal species. (B) Omitting the saturated range allowed us to capture the linear range of the standard curves, which were subsequently used for calculating NKA concentrations.

NKA detection is minimal to absent in negative controls

To assess the specificity of the antibodies used in the ELISA, several negative controls, which excluded different components of the ELISA, were tested. We set the detection threshold to 0.034, which is the average absorbance value of the reagents used in the ELISA (containing neither protein nor antibody). We found that the absorbance of the negative control containing no protein (i.e., membrane isolate) remained within this detection threshold (Fig. 5; Table S8). The negative control containing no HRP-conjugated secondary antibody fell slightly above this threshold. The negative control containing no primary α5-antibody minimally exceeded the detection threshold, which indicates that there is slight background noise caused by the HRP-conjugated secondary antibody. This is likely caused by unbound secondary antibody that remains in the well after repeated washing. In addition to these negative controls, we tested the NKA-specificity of the primary α5-antibody using membrane isolates of untransfected Sf9 cells, which express very little NKA endogenously [33,34]. There was some detection of NKAs in these membranes. This is expected because these cells express a small level of these proteins endogenously. In addition, untransfected cells have higher cell proliferation and thus membranes isolated from these samples will have a higher density of membranes than those isolated from transfected cells. Nevertheless, the detection of NKAs in samples derived from transfected Sf9 cells exceeded untransfected cells by more than two-fold (Fig. 5). Together, these results confirm that the specificity of the ELISA for NKA is suitable.
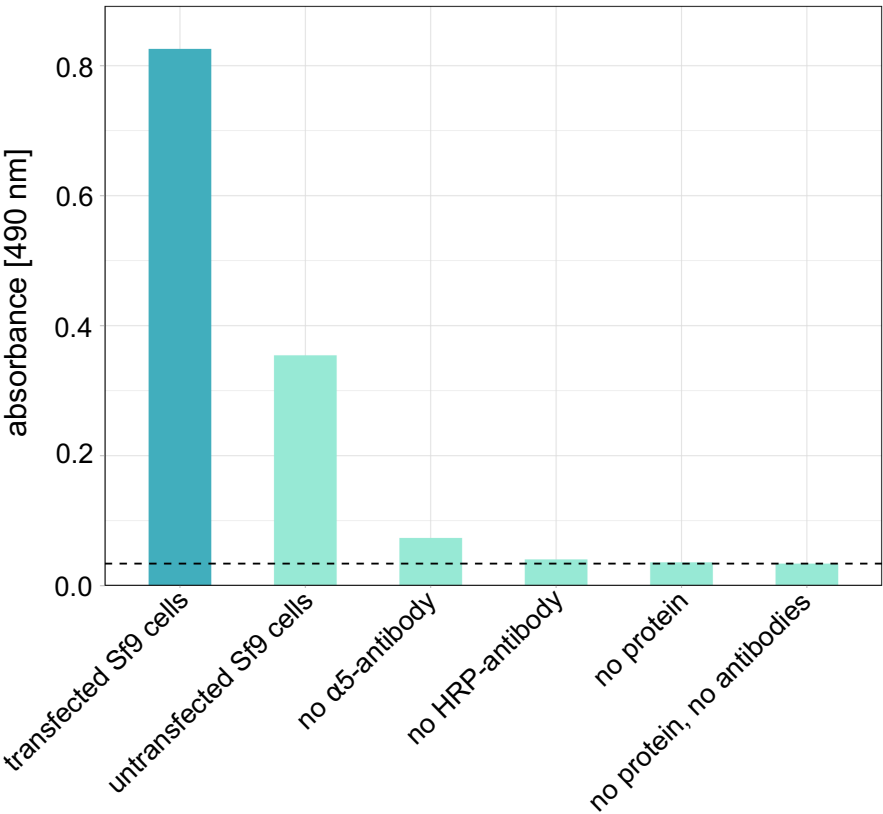

Figure 5. Comparison of absorbance values between a protein sample derived from transfected Sf9 cells (positive control; blue) and various negative controls (light turquoise). The positive control consisted of a gold tegu (replicate A) sample. This standard was subsequently used in the negative controls that contained protein (i.e., no α5-antibody and no HRP-antibody). The dashed line shows the

589 detection threshold of "no protein, no antibodies". Each bar represents the average of two technical
590 replicates from one biological replicate.
591
592 **Conventional protein quantification methods cannot sufficiently quantify NKA**
593
594 Our comparisons between protein quantification methods revealed several notable patterns (Fig. 6A).
595 In general, there was strong interspecies variation in protein concentrations among samples quantified
596 by ELISA, which ranged between 1.39 to 145.89 mg/mL. This variation was not as pronounced across
597 the samples quantified by conventional methods, which all-together ranged between 0.55 to 18.27
598 mg/mL (Supplementary Dataset 1). The absence of stark variation among the conventional
599 quantification methods strongly points towards their inability to robustly quantify NKA, and possibly
600 all transmembrane proteins.
601
602 Importantly, the positive control consisting of purified porcine NKA revealed that all three conventional
603 quantification methods determined protein concentrations much lower (<1.5 mg/mL) than its actual
604 concentration (10 mg/mL) (Fig. 6B; Supplementary Dataset 1). In contrast, the ELISA determined a
605 concentration 16.91 mg/mL, which is not only higher than the conventional methods but also exceeds
606 the predicted concentration based on lyophilized weight. All four quantification methods determined
607 approximately the same concentrations in the negative control consisting of membrane isolates from
608 untransfected Sf9 cells (Fig. 6B). Since untransfected cells have higher viability, the rather high
609 detected protein concentrations reflect the higher overall protein content resulting from higher cell
610 density. Taken together, these results suggest that the three conventional protein quantification
611 methods significantly underestimate the concentration of NKA in a given sample, and likely other large
612 transmembrane proteins.
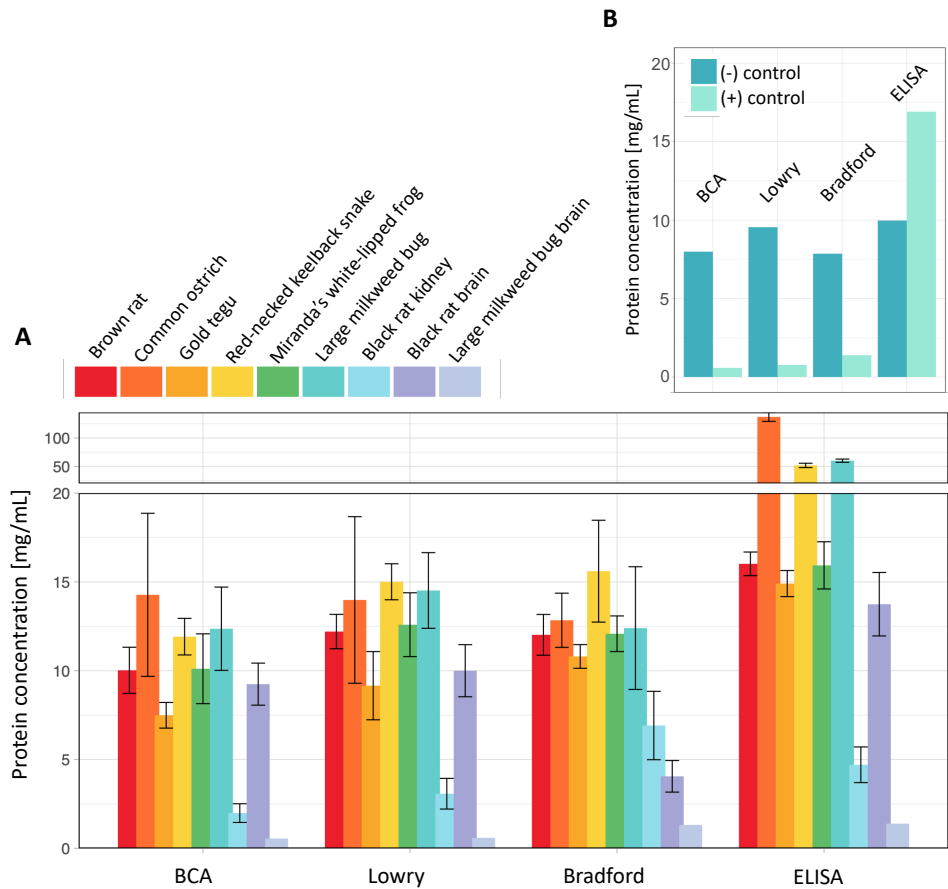
613
614 **Figure 6.** (A) Protein concentrations of recombinantly expressed and tissue-isolated NKAs. Bars
615 represent the mean and standard error of three biological replicates, with the exception of Miranda's

16

white-lipped frog and large milkweed bug brain, which consist of two and one replicates, respectively).
(B) Protein concentrations of the negative control (membrane isolates of untransfected Sf9 cells) and
positive control (commercial porcine sample) determined by the four quantification methods reveals
that the Lowry, BCA, and Bradford cannot sufficiently detect NKA.

To assess the NKA detection capabilities of the four different protein quantification methods, we
pooled the determined concentrations of each method and statistically compared the resulting
concentration distributions with the Friedman rank sum test for paired samples (Fig. 7A-B). We found
that the protein concentration distributions for recombinantly expressed proteins were significantly
different between the four methods (Friedman rank sum paired test; p < 0.001; χ2 = 36.53; df = 3; n =
15; Fig. 7A), with the ELISA having determined significantly higher protein concentrations compared to
all three conventional methods (Dunn's post-hoc test; Table S10). In contrast, the three conventional
methods did not significantly differ in their determined protein concentrations. Remarkably, the wide
range of NKA concentration differences detected by the ELISA was undetectable by the conventional
methods, which is clearly illustrated by the stark difference in box blots (Fig. 7A). This indicates that
using a transmembrane protein standard in place of the conventional BSA in the conventional methods
would not be effective. We also found a marginally significant difference in protein concentration
distributions for tissue-isolated samples (p = 0.006; χ2 = 12.6; df = 3; n = 9; Fig. 7B). However, a post-
hoc Dunn's test could not detect significant differences between any of the comparison pairs (Table
S10). We did not observe as wide a range of concentration differences in the ELISA on tissue samples.
This is likely due to tissue samples only covering two species (black rat and large milkweed bug).
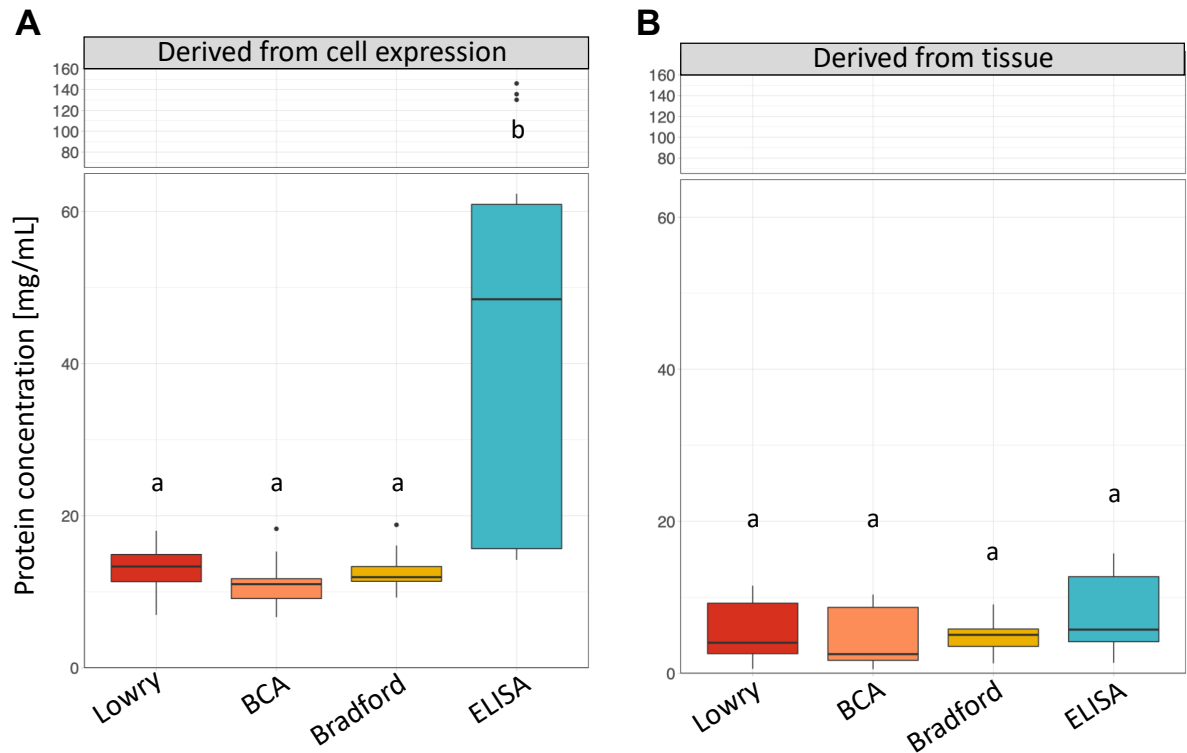
Figure 7. Comparison of protein concentrations determined by three conventional protein
quantification methods and the ELISA from (A) recombinantly expressed NKA and (B) tissue-isolated
proteins. Determined protein concentrations of different samples were pooled for each method. The
boxes show the 25% and 75% quantiles of the median (thick line), the whiskers represent the maximum
or minimum values without outliers. Outliers (filled-in circles) are protein concentrations greater or
less than 1.5 times the interquartile range. Sample sizes for all four methods: n = 17 (samples derived

646 from Sf9 cells) and n = 9 (nervous tissue and kidney isolates). Different letters indicate significant
647 differences in the distribution of determined protein concentrations at p < 0.05 (Dunn's test).
648
649 **Quantification with ELISA consistently produces more robust downstream ATPase assay data**
650
651 To test whether the differences in protein quantification accuracy we uncovered affect downstream
652 in vitro functional assays, ATPase activity assays were run based on protein concentrations determined
653 by the four quantification methods. We tested whether the resulting variation in NKA ATPase activities
654 (specified by standard deviation of NKA activity) significantly differs between the four quantification
655 methods.
656
657 We did not detect a significant effect of protein quantification method on the mean standard deviation
658 of NKA activities (ANOVA; p = 0.186; F = 1.882; n = 5; Fig. 8A). Although not statistically detectable, the
659 variation in NKA activities of all ELISA samples is consistently low compared to those of the
660 conventional methods, suggesting that the ELISA provides robust NKA quantification. Western blots of
661 the recombinantly expressed NKA show that expression levels were even across biological replicates
662 (Fig. S2). This indicates that overall protein content would be even within samples, and thus reduce
663 variation in activity based on concentrations determined by the conventional methods.
664
665 Of note, activity measurements of the large milkweed bug NKA resulted in stark differences between
666 the ELISA and conventional methods (Fig. 8B). The high activity associated with the conventional
667 methods is due to them detecting very low concentrations of the milkweed bug proteins, resulting in
668 more protein being added to the activity assay reaction, and subsequently higher measured activity.
669 In contrast, the ELISA detected rather high NKA concentrations in the large milkweed bug, which
670 resulted in less protein being used for the activity assays, and thus lower activity measurements. This
671 pattern can be seen across samples but is most pronounced in the milkweed bug.
672
673 In contrast to the Sf9 derived samples, the NKA activities of tissues derived samples deviate from this
674 pattern, showing high variation across all four quantification methods. Almost all the activity values of
675 tissue samples fell far beyond the linear range of the P_i standard curve. Thus, we could not make
676 accurate activity estimates for most of these samples. For this reason, they were excluded from the
677 ANOVA analysis.
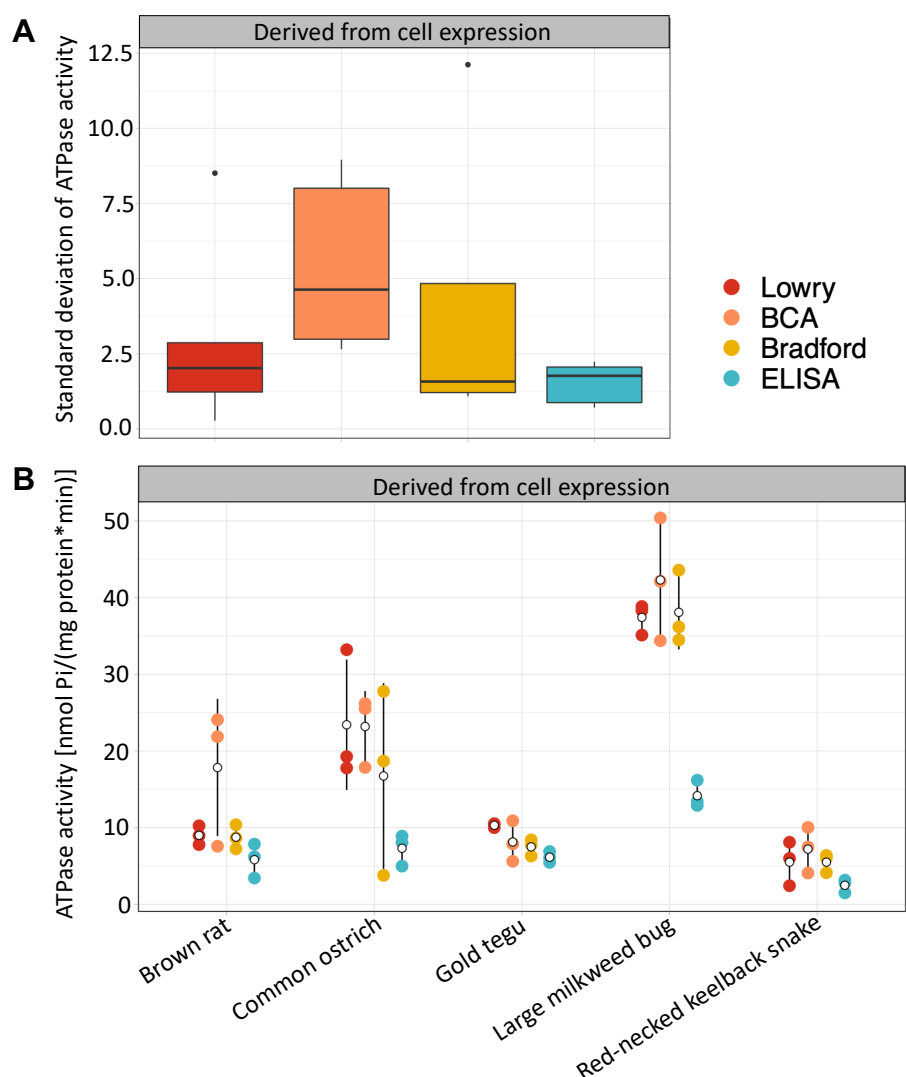
Figure 8. Comparison of the standard deviations (SDs) of Na, K-ATPase (NKA) ATPase activities measured based on protein concentrations determined by the four different protein quantification methods. (A) Pooled means showed no significant differences in SDs between the four methods. The box plots show the 25% and 75% quantiles of the median (thick line) and the maximum or minimum values without outliers (whiskers). Outliers (filled-in circles) are ATPase activities greater or less than 1.5 times the interquartile range. The sample size for each protein quantification method is n = 15. (B) Comparison of the variation in NKA activity of protein content calculated from concentrations determined by the four different protein quantification methods. Means and standard deviations of the three biological replicates are shown as hollow black circles and lines. Raw data points are shown as filled-in circles. Samples isolated from tissues were excluded from this analysis because activity levels fell beyond the linear range of standards.

4. Discussion

The overarching aim of this paper was to find a reliable method for quantifying large transmembrane proteins. We focused on the NKA as a model and we developed an ELISA that can be easily adapted across protein types and sources (i.e., species). We assessed the specificity of our ELISA in comparisons to commonly used conventional quantification methods (Lowry, BCA, and Bradford) and found that all conventional methods are unsuitable for quantifying NKA. If the conventional methods, which should detect all proteins in a given sample, quantify transmembrane proteins efficiently, then the protein

699 concentrations determined by these methods should be significantly higher than those determined by
700 the NKA-specific ELISA. Contrary to this expectation, we found that the ELISA consistently determined
701 higher protein concentrations in all the protein samples. Notably, the concentration of the positive
702 control, which consisted of pure NKA in membrane fragments, was grossly underestimated by the
703 conventional quantification methods—to the point where it was almost completely undetected (Fig.
704 6B). These outcomes are a clear indication that the Lowry, BCA, and Bradford assays cannot detect
705 transmembrane proteins. It is also important to point out that the ELISA also strongly underestimated
706 the concentration of the pure porcine NKA (Fig. 6B). This commercially available protein is purified
707 from porcine nervous tissue. According to the manufacturer, the primary α5-antibody, which we use
708 in the ELISA, is capable of binding to a cytosolic epitope on the NKA α-subunit of all isoforms across
709 the animal kingdom. However, it is possible that the α5-antibody binds more strongly to isoform α1
710 (ATP1A1), which we expressed in Sf9 cells, than to α3 (ATP1A3), which is the main isoform expressed
711 in nervous tissue [46]. To confirm this hypothesis, it would be prudent to test the antibody's ability to
712 detect α1 and α3 isoforms expressed and isolated from Sf9 cells.

713

714 There are several possible explanations for why the conventional quantification methods are
715 inefficient at detecting transmembrane proteins. We rule out interfering substances, such as
716 detergents, as a likely explanation for the inefficiency of the conventional methods because we used
717 HPLC grade water for the resuspension of isolated proteins. We can also rule out glycosylation as a
718 possible source of interference. Whereas glycosylation can lead to over- (Lowry and BCA) or
719 underestimation (Bradford) of protein concentrations [47] and the NKA β-subunit is highly glycolyzed,
720 our results consistently show underestimation of proteins by the conventional methods.

721

722 The most likely explanation has to do with the fact that the main detection molecules of the
723 conventional protein quantification methods, CBB and Cu^{2+}, are not able to penetrate the hydrophobic
724 cell membrane [21]. Isolated transmembrane proteins are embedded in membrane fragments and
725 therefore the embedded portion of the protein is not accessible to CBB and Cu^{2+} molecules, which bind
726 to specific amino acids on the protein surface. This would consequently result in underestimated
727 protein concentrations, and even more so considering that the protein standards for the conventional
728 methods consist of non-membrane proteins. Although penetrating the cell membrane should be less
729 of a barrier for the Lowry method because its alkaline reaction can disrupt cell membranes through
730 hydrolysis, the results did not show higher detectability by this method compared to the other two
731 (Fig. 7). In contrast, the α5-antibody of the ELISA binds to an epitope on the NKA α-subunit located
732 outside the cell membrane. Therefore, the detection pathway of the ELISA is not hindered by the
733 membrane and the resulting concentration measurement reflects a reliable estimate of the number of
734 NKA molecules in the sample. A possible alternative would be to produce the relative standards as
735 described for our ELISA and use them in conjunction with one of the conventional methods. However,
736 the very low detectability of our positive control by these methods casts doubts on whether a reliable
737 standard curve can be obtained with transmembrane proteins.

738

739 One unexpected outcome of these experiments is that all quantification methods detected lower
740 protein concentrations in the tissue-derived samples compared to the recombinantly expressed Sf9
741 cell-derived samples. It is possible that the lowered detection of proteins in tissue sample is due to
742 differences in the membrane composition, or co- and post-transcriptional modifications of Sf9 cells
743 and tissue cells, which might alter the accessibility of the epitope to the primary α5-antibody. In this
744 case, the tissue sample concentrations would also be lowered as a result of using relative standard
745 curves produced from Sf9 cell derived NKA. The stark difference in detectability of rat NKA from
746 recombinantly expressed Sf9 cells and from kidney tissue, both of which consist of the rat isoform α1
747 (ATP1A1), supports this hypothesis.

748

749 The NKA activity assays, which were run based on protein concentrations determined by the different
750 quantification methods, helped to serve as an additional robustness assessment of the methods. The

751 activity data of Sf9 cell-derived NKA showed consistently low variation across all animal species when
752 the NKA activity assays were based on ELISA-determined protein concentrations (Fig. 8). The NKA
753 activity assays based on concentrations determined by the three conventional methods exhibited
754 different levels of variation across animal species—meaning that some animal species exhibited low
755 variation in NKA activities while others exhibited high variation (Fig. 8). Due to these overlaps, it was
756 not possible to detect a statistical difference between NKA activity variation in ELISA-based and other
757 quantification method-based data. According to the ELISA, the determined NKA concentrations of
758 protein samples derived from Sf9 cells were quite similar across the three biological replicates of each
759 animal species. The conventional methods determined protein concentrations that were considerably
760 lower, but, as with ELISA, they differ only slightly across biological replicates. This, in turn, resulted in
761 lower variation in NKA activities for the conventional methods. The even NKA expression across
762 biological replicates, as seen on the western blots (Fig. S2), further corroborate why no statistical
763 difference was detected in the NKA activity variation between the four protein quantification methods.
764 If NKA expression levels were uneven across biological replicates, then we would have expected to see
765 more variation in the resulting activity data based on the conventional methods.

767 Of note, we found that the NKA activity assays of tissue-derived samples exhibited very high variation
768 across the board. This was likely due to the absorbance values measured for the activity assays
769 exceeding the linear range of the P_i standard curve, making accurate quantification of phosphate
770 released from the hydrolysis of ATP impossible. There are two possible explanations for this outcome.
771 The first is that NKAs derived from tissue have a higher catalytic activity than those expressed
772 recombinantly. When the NKA activity is very high, then considerably less protein would be needed in
773 the NKA activity assay to fall within the detectable range of the standard curve. Another explanation
774 is that all four quantification methods, including the ELISA, severely underestimated the total NKA
775 concentrations in tissue-derived samples, as was discussed previously. When the NKA concentration is
776 underestimated, then more protein is used in the NKA activity assay, driving the NKA activity levels
777 beyond the linear range of the standard curve. Despite numerous rounds of dilutions, we were never
778 able to capture activity levels that fell within the standards range for our tissue-derived samples.

780 As part of the functional validation of the ELISA, several negative controls were run to test non-specific
781 background noise in the ELISA. The negative control containing only NKA and the secondary HRP-
782 antibody ("no α5-antibody") showed a slightly higher absorbance than the detection threshold (Fig. 5).
783 This minimal background noise most likely results from HRP-antibodies that remain in the wells after
784 washing. For this reason, the number of wash steps following HRP-antibody incubation is higher than
785 the rest of the washing steps. The absorbances of the other negative controls containing no HRP-
786 conjugated secondary antibody or no protein sample did not exceed the detection threshold,
787 indicating that TMB and the stopping solution do not stain non-specifically and that non-specific
788 binding of the antibodies to the wells is not an issue in this ELISA**.**

790 Another important validation step involved confirming by western blot and ELISA that lyophilization
791 does not alter the detectability of NKA by the antibodies used in the ELISA, thereby ensuring that the
792 standards will not be detected differently than the fresh protein samples. Verifying that lyophilized cell
793 membrane isolates can be used to produce relative protein standards is important considering how
794 different the relative NKA standard curves can look for different animal species (Fig. 4). Without
795 producing a standard curve for each animal species, the determined NKA concentrations would be
796 biased towards the detectability of the protein's animal species origin and thus significantly over- or
797 underestimate NKA content in different samples. These interspecies differences are due to the α5-
798 antibody binding at different efficiencies with different animal species (Fig. 4; Fig. S2).

800 Overall, our results indicate that the ELISA is the most suitable quantification method for the NKA, and
801 most likely other large transmembrane proteins as well. The ELISA validated here can be easily adapted
802 to other transmembrane proteins by exchanging the primary and, if necessary, the secondary

803 antibody. Moreover, it is straightforward to prepare relative protein standards that can be adapted to
804 a wide taxonomic range and multiple sample types. This method eliminates the need for commercially
805 available ELISA kits, which are more limited in these regards and can be quite costly.
806
807 **Acknowledgements**
808

6. References

1. Mohammadi S, Herrera-Álvarez S, Yang L, del Pilar Rodríguez-Ordoñez M, Zhang K, Storz JF, Dobler S, Crawford AJ, Andolfatto P. 2022 Constraints on the evolution of toxin-resistant Na,K-ATPases have limited dependence on sequence divergence. *PLoS genetics* **18**, e1010323. (doi:10.1371/journal.pgen.1010323)

2. Dalla S, Baum M, Dobler S. 2017 Substitutions in the cardenolide binding site and interaction of subunits affect kinetics besides cardenolide sensitivity of insect Na, K-ATPase. *Insect biochemistry and molecular biology* **89**, 43–50.

3. Orlowski J, Lingrel JB. 1988 Tissue-specific and developmental regulation of rat Na, K-ATPase catalytic alpha isoform and beta subunit mRNAs. *Journal of Biological Chemistry* **263**, 10436–10442.

4. Ahrens H *et al.* 2015 siRNA mediated knockdown of tissue factor expression in pigs for xenotransplantation. *American journal of transplantation* **15**, 1407–1414.

5. Lowry O, Rosebrough N, Farr AL, Randall R. 1951 Protein measurement with the Folin phenol reagent. *Journal of biological chemistry* **193**, 265–275.

6. Smith PK *et al.* 1985 Measurement of protein using bicinchoninic acid. *Analytical Biochemistry* **150**, 76–85. (doi:10.1016/0003-2697(85)90442-7)

7. Bradford MM. 1976 A rapid and sensitive method for the quantitation of microgram quantities of protein utilizing the principle of protein-dye binding. *Analytical Biochemistry* **72**, 248–254. (doi:10.1016/0003-2697(76)90527-3)

8. Fanger BO. 1987 Adaptation of the Bradford protein assay to membrane-bound proteins by solubilizing in glucopyranoside detergents. *Analytical Biochemistry* **162**, 11–17. (doi:10.1016/0003-2697(87)90004-2)

9. Mehl JW, Pacovska E, Winzler RJ. 1949 The amount of copper bound by protein in the biuret reaction. *Journal of Biological Chemistry* **177**, 13–21.

10. Legler G, Müller-Platz CM, Mentges-Hettkamp M, Pflieger G, Jülich E. 1985 On the chemical basis of the Lowry protein determination. *Analytical Biochemistry* **150**, 278–287. (doi:10.1016/0003-2697(85)90511-1)

11. Everette JD, Bryant QM, Green AM, Abbey YA, Wangila GW, Walker RB. 2010 Thorough Study of Reactivity of Various Compound Classes toward the Folin–Ciocalteu Reagent. *J. Agric. Food Chem.* **58**, 8139–8144. (doi:10.1021/jf1005935)

12. Stoscheck CM. 1990 [6] Quantitation of protein. In *Methods in Enzymology* (ed MP Deutscher), pp. 50–68. Academic Press. (doi:10.1016/0076-6879(90)82008-P)

13. Wiechelman KJ, Braun RD, Fitzpatrick JD. 1988 Investigation of the bicinchoninic acid protein assay: Identification of the groups responsible for color formation. *Analytical Biochemistry* **175**, 231–237. (doi:10.1016/0003-2697(88)90383-1)

14. Noble JE, Bailey MJA. 2009 Chapter 8 Quantitation of Protein. In *Methods in Enzymology* (eds RR Burgess, MP Deutscher), pp. 73–95. Academic Press. (doi:10.1016/S0076-6879(09)63008-1)

852   15. Georgiou CD, Grintzalis K, Zervoudakis G, Papapostolou I. 2008 Mechanism of Coomassie brilliant
853   blue G-250 binding to proteins: a hydrophobic assay for nanogram quantities of proteins.
854   *Analytical and Bioanalytical Chemistry* **391**, 391–403. (doi:10.1007/s00216-008-1996-x)

855   16. Reinmuth-Selzle K *et al.* 2022 Determination of the protein content of complex samples by
856   aromatic amino acid analysis, liquid chromatography-UV absorbance, and colorimetry. *Analytical*
857   *and Bioanalytical Chemistry* **414**, 4457–4470.

858   17. Friedenauer S, Berlet HH. 1989 Sensitivity and variability of the Bradford protein assay in the
859   presence of detergents. *Analytical Biochemistry* **178**, 263–268. (doi:10.1016/0003-
860   2697(89)90636-2)

861   18. Compton SJ, Jones CG. 1985 Mechanism of dye response and interference in the Bradford
862   protein assay. *Analytical Biochemistry* **151**, 369–374. (doi:10.1016/0003-2697(85)90190-3)

863   19. Carpenter EP, Beis K, Cameron AD, Iwata S. 2008 Overcoming the challenges of membrane
864   protein crystallography. *Current Opinion in Structural Biology* **18**, 581–586.
865   (doi:10.1016/j.sbi.2008.07.001)

866   20. Trötschel C, Poetsch A. 2015 Current approaches and challenges in targeted absolute
867   quantification of membrane proteins. *PROTEOMICS* **15**, 915–929. (doi:10.1002/pmic.201400427)

868   21. Kirazov LP, Venkov LG, Kirazov EP. 1993 Comparison of the Lowry and the Bradford Protein
869   Assays as Applied for Protein Estimation of Membrane-Containing Fractions. *Analytical*
870   *Biochemistry* **208**, 44–48. (doi:10.1006/abio.1993.1006)

871   22. Cienfuegos-Jiménez O, Morales-Hernández A, Robles-Rodríguez OA, Bustos-Montes S, Bañuelos-
872   Alduncin KA, Cortés-Castillo AR, Barreto-Hurtado HD, Carrete-Salgado L, Marino-Martínez IA.
873   2022 High-yield production and purification of the fusion pH-responsive peptide GST-pHLIP in
874   Escherichia coli BL21. *AIMS Molecular Science* **9**, 136–144. (doi:10.3934/molsci.2022008)

875   23. AU - Yadavalli R, AU - Sam-Yellowe T. 2015 HeLa Based Cell Free Expression Systems for
876   Expression of Plasmodium Rhoptry Proteins. *JoVE* , e52772. (doi:10.3791/52772)

877   24. Dobler S, Wagschal V, Pietsch N, Dahdouli N, Meinzer F, Romey-Glüsing R, Schütte K. 2019 New
878   ways to acquire resistance: imperfect convergence in insect adaptations to a potent plant toxin.
879   *Proc Biol Sci* **286**, 20190883. (doi:10.1098/rspb.2019.0883)

880   25. Karageorgi M *et al.* 2019 Genome editing retraces the evolution of toxin resistance in the
881   monarch butterfly. *Nature* **574**, 409–412. (doi:10.1038/s41586-019-1610-8)

882   26. Mohammadi S *et al.* 2021 Concerted evolution reveals co-adapted amino acid substitutions in
883   Na+K+-ATPase of frogs that prey on toxic toads. *Curr Biol* **31**, 2530-2538.e10.
884   (doi:10.1016/j.cub.2021.03.089)

885   27. Engvall E, Perlmann P. 1972 Enzyme-linked immunosorbent assay, ELISA: III. Quantitation of
886   specific antibodies by enzyme-labeled anti-immunoglobulin in antigen-coated tubes. *The Journal*
887   *of Immunology* **109**, 129–135.

888   28. Gan SD, Patel KR. 2013 Enzyme immunoassay and enzyme-linked immunosorbent assay. *Journal*
889   *of Investigative Dermatology* **133**, 1–3.

890   29. Walker JM, Crowther J. 2009 The ELISA guidebook. In *Series Springer Protocols. Methods in*
891   *Molecular Biology*, Springer.

892   30. Kaplan JH. 2002 Biochemistry of Na,K-ATPase. *Annu. Rev. Biochem.* **71**, 511–535.
893   (doi:10.1146/annurev.biochem.71.102201.141218)

894   31. Scheiner-Bobis G. 2002 The sodium pump: Its molecular properties and mechanics of ion
895   transport. *European journal of biochemistry* **269**, 2424–2433.

896   32. Herbertz M, Dalla S, Wagschal V, Turjalei R, Heiser M, Dobler S. 2023 Co-evolutionary escalation
897   led to differentially adapted paralogs of an insect's Na,K-ATPase optimizing resistance to host
898   plant toxins. *Molecular Ecology*

899   33. Blanco G, Xie ZJ, Mercer RW. 1993 Functional expression of the alpha 2 and alpha 3 isoforms of
900   the Na, K-ATPase in baculovirus-infected insect cells. *Proceedings of the National Academy of*
901   *Sciences* **90**, 1824–1828.

902   34. DeTomaso AW, Xie ZJ, Liu G, Mercer R. 1993 Expression, targeting, and assembly of functional
903   Na, K-ATPase polypeptides in baculovirus-infected insect cells. *Journal of Biological Chemistry*
904   **268**, 1470–1478.

905   35. Scholz J, Suppmann S. 2017 A new single-step protocol for rapid baculovirus-driven protein
906   production in insect cells. *BMC biotechnology* **17**, 1–9.

907   36. Herbertz M, Harder S, Schlüter H, Lohr C, Dobler S. 2022 Na, K-ATPase α1 and β-subunits show
908   distinct localizations in the nervous tissue of the large milkweed bug. *Cell and Tissue Research* ,
909   1–17.

910   37. Lohr JN, Meinzer F, Dalla S, Romey-Glüsing R, Dobler S. 2017 The function and evolutionary
911   significance of a triplicated Na, K-ATPase gene in a toxin-specialized insect. *BMC evolutionary*
912   *biology* **17**, 1–10.

913   38. Yu Y *et al.* 2014 A rat RNA-Seq transcriptomic BodyMap across 11 organs and 4 developmental
914   stages. *Nature communications* **5**, 3230.

915   39. Yue F *et al.* 2014 A comparative encyclopedia of DNA elements in the mouse genome. *Nature*
916   **515**, 355–364.

917   40. Djamgoz M, Ready P, Billingsley P, Emery A. 1998 Insect Na (+)/K (+)-ATPase. *Journal of Insect*
918   *Physiology* **44**, 197–210.

919   41. Petschenka G, Fandrich S, Sander N, Wagschal V, Boppré M, Dobler S. 2013 Stepwise evolution of
920   resistance to toxic cardenolides via genetic substitutions in the Na+/K+ -ATPase of milkweed
921   butterflies (lepidoptera: Danaini). *Evolution* **67**, 2753–2761. (doi:10.1111/evo.12152)

922   42. Taussky HH, Shorr E. 1953 A microcolorimetric method for the determination of inorganic
923   phosphorus. *J Biol Chem* **202**, 675–685.

924   43. Schneider CA, Rasband WS, Eliceiri KW. 2012 NIH Image to ImageJ: 25 years of image analysis.
925   *Nature Methods* **9**, 671–675. (doi:10.1038/nmeth.2089)

926   44. Kassambara A. 2023 Pipe-Friendly Framework for Basic Statistical Tests [R package rstatix version
927   0.7. 2]. Comprehensive R Archive Network (CRAN).

928   45. Champely S, Ekstrom C, Dalgaard P, Gill J, Weibelzahl S, Anandkumar A, Ford C, Volcic R, De
929   Rosario H. 2017 pwr: Basic functions for power analysis.

930   46. Bøttger P, Tracz Z, Heuck A, Nissen P, Romero-Ramos M, Lykke-Hartmann K. 2011 Distribution of
931   Na/K-ATPase alpha 3 isoform, a sodium-potassium P-type pump associated with rapid-onset of
932   dystonia parkinsonism (RDP) in the adult mouse brain. *Journal of Comparative Neurology* **519**,
933   376–404. (doi:10.1002/cne.22524)

934   47. Fountoulakis M, Juranville J-F, Manneberg M. 1992 Comparison of the Coomassie brilliant blue,
935   bicinchoninic acid and Lowry quantitation assays, using non-glycosylated and glycosylated
936   proteins. *Journal of Biochemical and Biophysical Methods* **24**, 265–274. (doi:10.1016/0165-
937   022X(94)90078-7)

938